frontiers | Frontiers in Earth Science

ORIGINAL RESEARCH
published: 02 June 2022
doi: 10.3389/feart.2022.911123

Drilling Cores and Geophysical Characteristics of Gas Hydrate-Bearing Sediments in the Production Test Region in the Shenhu sea, South China sea

Jin Liang[1,2,3], *Miaomiao Meng*[1,2,3]*, *Jinqiang Liang*[1,2,3], *Jinfeng Ren*[1,2,3]*, *Yulin He*[1,2,3], *Tingwei Li*[1,2,3], *Mengjie Xu*[1,2,3] *and Xiaoxue Wang*[1,2,3]

[1]*Southern Marine Science and Engineering Guangdong Laboratory (Guangzhou), Guangzhou, China,* [2]*MLR Key Laboratory of Marine Mineral Resources, Guangzhou Marine Geological Survey, Ministry of Natural Resources, Guangzhou, China,* [3]*National Engineering Research Center of Gas Hydrate Exploration and Development, Guangzhou, China*

OPEN ACCESS

Edited by:
Jinan Guan,
Chinese Academy of Sciences (CAS), China

Reviewed by:
Qinggguo Meng,
Qingdao Institute of Marine Geology (QIMG), China
Qinghai Xu,
Yangtze University, China

***Correspondence:**
Miaomiao Meng
18811309981@126.com
Jinfeng Ren
jf_ren@163.com

Specialty section:
This article was submitted to Marine Geoscience, a section of the journal Frontiers in Earth Science

Received: *02 April 2022*
Accepted: *02 May 2022*
Published: *02 June 2022*

Citation:
Liang J, Meng M, Liang J, Ren J, He Y, Li T, Xu M and Wang X (2022) Drilling Cores and Geophysical Characteristics of Gas Hydrate-Bearing Sediments in the Production Test Region in the Shenhu sea, South China sea. Front. Earth Sci. 10:911123. doi: 10.3389/feart.2022.911123

Gas hydrate production testing was conducted in 2017 in the Shenhu Area in the northern part of the South China Sea, and unprecedented success was achieved. In order to obtain gas production and physical properties of gas hydrate reservoirs in the study area and determine the location of test production wells, the seismic and logging data and drilling cores were analyzed in detail, the physical characteristics of the sediments, faults, gas components, and reservoir were studied. The results show that 1) the gas hydrates are diffusion type, with reservoirs dominated by clayey silt sediments, and the gas hydrate-bearing layers are characterized by soup-like, porridge-like, cavity, and vein structures; 2) the resistivity and acoustic velocity of gas hydrate formation are significantly higher than those of the surrounding sediments, while the neutron porosity, density, and natural gamma are slightly lower; the Bottom Simulating Reflectors (BSRs) in seismic profiles exhibit the exist of gas hydrates; 3) gas chimneys and faults are well-developed beneath the BSRs, and hydrocarbon gases can easily migrate into the gas hydrate reservoirs in areas with stable temperature and pressure conditions; 4) the gas hydrate saturation is high, the highest saturation in site W17 was up to 76%, with an average of 33%; while the highest saturation in site W19 was up to 68%, with an average of 31%. The gas source is considered as mixed gas of thermogenic gas and microbial gas. By comparing the core samples and geophysical characteristics of sites W17 and W19 in the study area and calculating the thickness, distribution area, and saturation of the hydrate deposition layer, it was found that site W17 is characterized by a thick layer, large area, high saturation, and good sealing, and thus, site W17 was established as the test production site. The development of gas chimney and faults provides pathways for the upward migration of deep gas, and the gas migrates to gas hydrate stable zone in forms of diffusion, water soluble and free state, forming high saturation of diffusion gas hydrates.

Keywords: gas hydrates, gas hydrate-bearing sediments, geophysical characteristics, saturation, gas source

INTRODUCTION

Natural gas hydrates (hereinafter referred to as hydrates) mainly exist in the shallow sedimentary strata in marine continental margins and permafrost regions in alpine areas on land (Kvenvolden and Lorenson, 2001; Collett, 2002, 2010; Klauda and Sandier, 2005; Demirbas, 2010; Chong et al., 2016). Under high pressure and low-temperature conditions, they are cage structure compounds composed of an ice lattice and adsorbed natural gas molecules (Booth et al., 1994; Wang et al., 2006; Wang et al., 2014). In recent years, gas hydrate reservoirs closely related to levee facies have been discovered by exploration or drilling in several sea areas around the world (Boswell et al., 2012; Lee and Collett, 2012).

At present, the geophysical characteristics of hydrate-bearing sediments has been studied by many experts and scholars (Liang et al., 2013; Yu et al., 2014). Compared with the surrounding unconsolidated sediments, pure hydrates are considered to have the physical properties of a high acoustic velocity and resistivity and low density. The high acoustic velocity of hydrates changes the seismic reflection characteristics of the sedimentary strata, forming a strong amplitude Bottom Simulating Reflector (BSR), weak amplitude blank zone, and bottom reverse polarity from that of the seafloor on seismic reflection profiles (Wang et al., 2005; Liang et al., 2014). Under the sufficient gas supply, suitable migration channels, and storage space, the distribution of natural gas hydrate stability zone is only related to the temperature and pressure of the sedimentary strata. Therefore, when the sedimentary strata are inclined on the continental slope or in the shallow seabed, the BSR on the seismic profile usually obliquely crosses the sedimentary strata (Paull et al., 1991; Kvenvolden, 1993; Liang et al., 2016). On the logging curve, gas hydrate-bearing strata usually has obvious high resistivity and high acoustic velocity (Hyndman and Davis, 1992; Liang et al., 2013). In addition, since gas hydrates are usually formed in sedimentary layers with relatively large pores, the neutron porosity is slightly higher and the spontaneous potential value is relatively small (Kawasaki et al., 2011; Boswell et al., 2012; Lee and Collett, 2012). The density of hydrate-bearing formations is usually only slightly lower, but for relatively pure and massive hydrates, the density log value can be significantly lower (Lee et al., 1993; Walter et al., 1999; Liang et al., 2006). These results play a guiding role in general surveys and detailed surveys of hydrates, but due to the limitations of the available data (usually only seismic data and a small amount of logging data), and the lack of verification of cores, lithologic interpretation has the limitation of multiple solutions, and the gas hydrate occurrences cannot be finely characterized. Therefore, it is hard to accurately determine the experimental exploitation wells of natural gas hydrates.

In 2015, gas hydrate drillings were carried out before production test in the Shenhu area of the northern South China Sea. Logging while drilling was conducted at 19 drilling sites, and *in situ* measurements and coring were conducted at four sites. The logging data show that gas hydrates with different saturation were developed in the 19 sites. High saturation and very thick diffusion hydrate samples were acquired from the four drilling sites (Yang et al., 2015, Yang et al., 2017 S. X.; Zhong et al., 2017; Zhang et al., 2018).

In 2017, test drilling in the Shenhu area in the northern South China Sea were conducted by Guangzhou Marine Geological Survey. This test produced 309000 m^3 gas, with average daily gas production of more than 5000 m^3 and methane content of up to 99.5%. Before the location of production test drilling was determined, the lithological characteristics, vertical variation of gas hydrate-bearing sedimentary strata, gas hydrate saturation, reservoir thickness, and gas source should be cleared. Through detailed analysis of pressure cores and 3-D seismic and geophysical well logging data, gas hydrate-bearing sediments were finely characterized, overcoming the limitations and interpretation ambiguity that exist when only geophysical data are used and revealing the physical properties and storage characteristics of the hydrate-bearing sedimentary strata. The gas migration and accumulation characteristics were studied based on the regional geological structure and metallogenic conditions, and the location of the test well was finally determined. The great success of the production test verified the accuracy of the interpretation of the geophysical characteristics of gas hydrate-bearing sediments.

GEOLOGICAL SETTING

The study area is located in the continental slope zone in the Shenhu area in the northern part of the South China Sea (**Figure 1**), with a water depth range of 350–1750 m. The water depth contours are roughly parallel to the coastline. The measured heat flow in the Shenhu area is about 60–96 mW/m^2, and the average heat flow is about 76 mW/m^2. Compared with the heat flow in the Pearl River Mouth Basin in the northern part of the South China Sea, the average heat flow in the Shenhu area is about 5–6 mW/m^2 higher than those in the southern depression and central uplift in the Pearl River Mouth Basin, indicating that the hydrothermal activity within the deep strata in the Shenhu area is relatively active, and the velocity of the fluid migration in the strata is relatively fast. The seafloor temperature in the study area is about 2–4°C, the geothermal gradient of the seafloor sediments is about 46–68°C/km, and the water depth pressure of the seafloor is greater than 10 MPa. Therefore, the conditions of the hydrate accumulation in the study area are relatively stable (Zhang et al., 2017). The seafloor topography in the study area fluctuates greatly and the changes are relatively complex. The slope of the seafloor decreases slowly from north to south, and the average value of the sea floor slope gradient is about 18‰. Under the joint impact of the gravity current and submarine current, a submarine landslide is relatively well-developed in the study area, which is manifested by the alternating arrangement of dunes and troughs, forming a pattern of scour trenches and submarine ridges spreading in a nearly north-south direction. The formation and decomposition of the gas hydrates are closely related to the submarine landslide. The landslide is a favorable geological body for the formation and distribution of gas hydrates. The large amount of water and gas released during the decomposition of gas hydrates, which could result in the instability of the overlying strata and accelerates the submarine landslide.

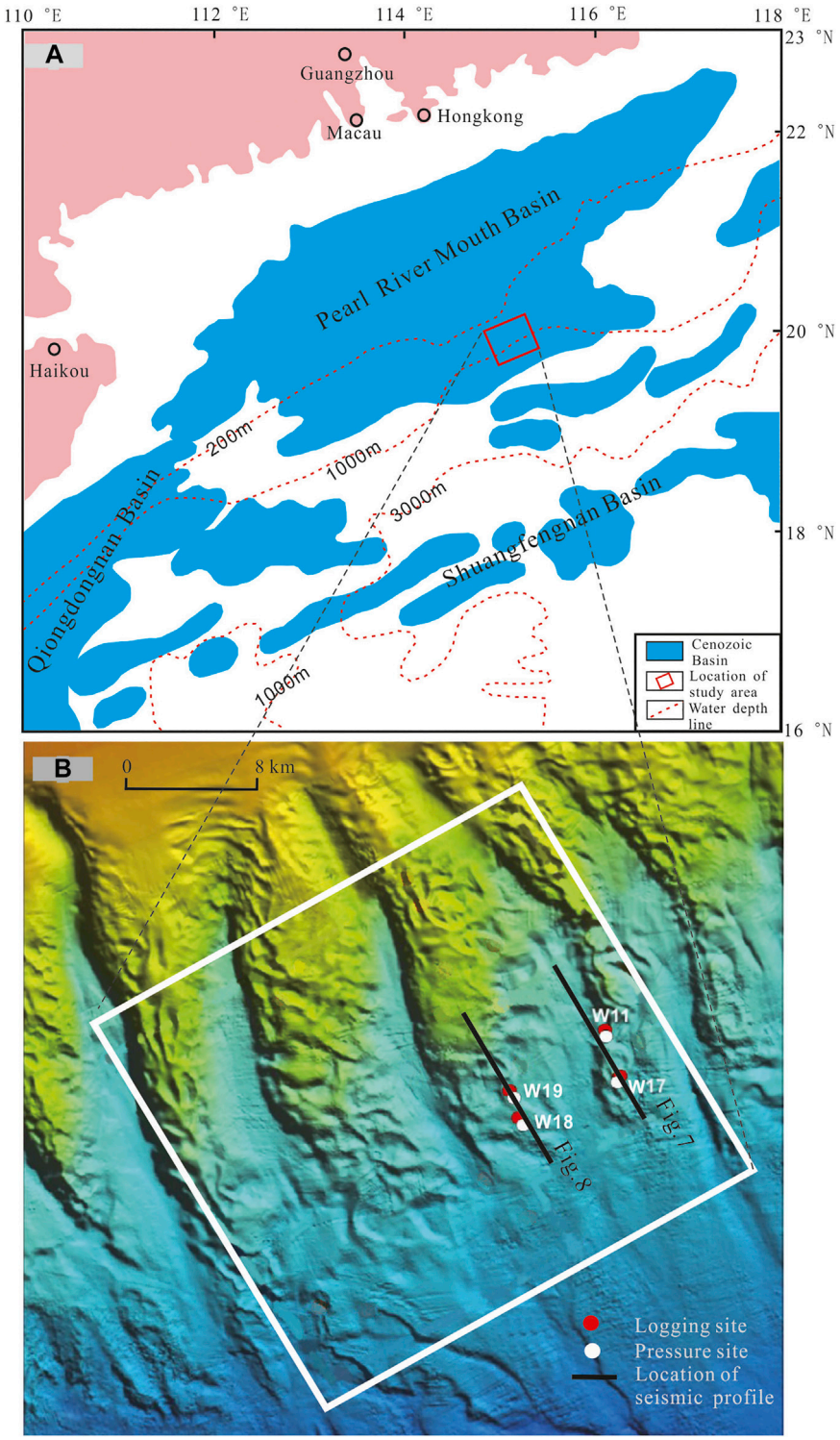

FIGURE 1 | Location of production testing and drilling sites in the pearl river mouth basin, south china sea. Note: the two black lines show the location of seismic profiles in **Figures 7**, **8** respectively.

There is an excellent correspondence between the seabed landslide and BSRs in the study area, and the BSRs can be seen clearly at the bottom of the landslide. The extremely high sedimentation rate in the Shenhu Sea area has resulted in a very thick sedimentary layer. The research area is located in the Baiyun Depression, which has a large area and a very thick sedimentary

layer. It is the main hydrocarbon generation and expulsion depression in the Shenhu area, with TOC content in the range of 0.50–1.52%, and Ro content in the range of 0.6–1.3%, and it has very favorable conditions for the formation of hydrates. The upper strata in the study area are mainly argillaceous deposits with relatively low sand contents, high organic matter contents, and low thermal maturity. Therefore, large quantities of biogas are easily generated, and hydrate orebodies can be formed under certain temperature and pressure conditions. Neritic detrital and bathyal clastic sedimentary substrata are relatively well-developed. Their sediment organic matter contents are higher. The organic matter in the eastern Pearl River Mouth Basin near the study area is in mature or highly mature stage (Ro = 1.3–2.5%), and in the local area, the organic matter has entered the overly mature stage. This has resulted in oil and gas formation (i.e., cracking gas and thermogenic gas), providing abundant thermogenic gas for hydrate formation (Zhang et al., 2014; He et al., 2008; 2013). In addition, the neotectonic movement led to the plastic flow of thick over pressurized mud, forming a large-scale diapir active zone, resulting in the abnormal development of mud diapirs, gas chimneys, faults and vertical fissures, and providing favorable gas-bearing fluid migration and transport channels for gas hydrate formation in the study area (He et al., 2014; Zhang et al., 2017).

DATA AND METHODS

In 2015, Logging While Drilling (LWD) was conducted at 19 drilling sites by the China Geological Survey (CGS) in the hydrate production test area in the Shenhu Sea, and pressure coring was conducted at 4 sites (**Figure 1**). The logging parameters mainly included resistivity, bit resistivity imaging, p-wave acoustic time difference, full-wave logging and neutron, density, well diameter, and natural gamma logging. After the sample coring, *in-situ* temperature and formation pore pressure dispersion tests were performed. The geochemical analysis of the samples was conducted in the field. The logging data revealed that various amounts of gas hydrates existed in the 19 sites, and the core samples directly proved that gas hydrates filled the pore spaces of the formation in the study area. Among the 19 sites, sites W11, W17, and W19 have the most obvious gas hydrate characteristics. Sites W11 and W17 are located close to each other and have similar geophysical properties. In this study, sites W17 and W19 were taken as examples to analysis the logging characteristics of gas hydrates. In addition, the quasi-3-D seismic data collected by the Fendou 4 (research vessel) in the research area in 2008 were used. The original surface element size was 12.5 m × 50 m, the number of receiving channels was 192, the channel spacing was 12.5 m, the gun spacing was 25 m, the minimum offset was 125 m, the sampling rate was 1 ms, the recording length was 5 s, and the cable and source-sink depth was 5 m. The Source capacity was 160 Cu. in, and the working pressure was 2000 Psi. In terms of seismic data processing for gas hydrate characteristics, prestack noise suppression, deconvolution and multiple wave suppression are mainly used to achieve high SNR, high resolution and high fidelity processing effect.

RESULTS

Characteristics of Gas Hydrate-Bearing Sediments

Through the observation of drilling cores, it was found that gas hydrates are closely related to the medium-coarse sediments and fractures. The high saturation gas hydrates mainly occur as pore-filling, blocky, and vein forms in the medium-coarse sediments and small fractures. However, the core and lithological analysis of sediment samples from the study area indicates that gas hydrates accumulated and occur in the fine-grained sediments, and the gas hydrates are uniformly distributed within the sediments (**Figures 2**, **3**). The gas hydrate-bearing sediments can be divided into four lithologic types: siliceous-bearing calcareous clayey silt, calcareous and siliceous-bearing clayey silt, calcareous silt, and calcareous clayey silt. Most of the free gas accumulates in the gas hydrate stability zone in the form of diffuse deposits, and a small part migrates along the faults. In the study area, gas chimneys are developed below the BSR, but the faults are not developed above the BSR, so diffusive gas hydrates are easily formed. Shallow biogenic gas and deep thermogenic gas enters the bottom of the hydrate stability zone, and then, they diffuse and are stored in the sediment pores. Because there are no fractures, it is easy for a stable gas hydrate accumulation area with an uneven distribution to form. The core samples from 1465 to 1475 m (water depth) and core infrared images taken at 1490–1510 m in site W17 (**Figure 2**) show that the main lithology is calcareous clay medium-coarse silt, and the hydrates in this depth interval often occur as dispersed fine particles. The sedimentary structures include vein, soup-like, and porridge-like occurrences (**Figure 2**). Low temperature anomalies (10–12°C) were observed in the core samples due to hydrate decomposition. The gas hydrates are evenly distributed in the sediment pore space. **Figure 3** shows core samples from 1418 to 1426 m (water depth) in site W19 and the core infrared image was taken at 1424–1438 m. Strong gas swelling phenomenon and cavity and congee core structures formed during the decomposition of the hydrates were observed after the cores arrived in the lab. The core from this section was obtained from the gas hydrate enrichment layer. Through pressure relief and degassing treatment, a large amount of gas was collected. The infrared image scanning of the core revealed a low temperature region (10–12°C) with a geothermal gradient of 5.58°C/100 m. The core from site W19 is mainly composed of calcareous nodular silt. The gas migrated upward through the migration channels formed by the gas chimneys, and abundant inorganic substances were gathered in this area, which promoted the enrichment of microorganisms and other calcium-rich substances, forming calcareous nodular silt.

The chemical properties and gas sources of hydrates are reflected by the gas composition and carbon isotopic characteristics of the gas hydrates (Chen et al., 2002; Fu et al., 2011; Fang et al., 2019). The methane contents of the gas samplesare greater than 98.5%, while ethane and propane are about 1 and 0.5%, respectively, but high

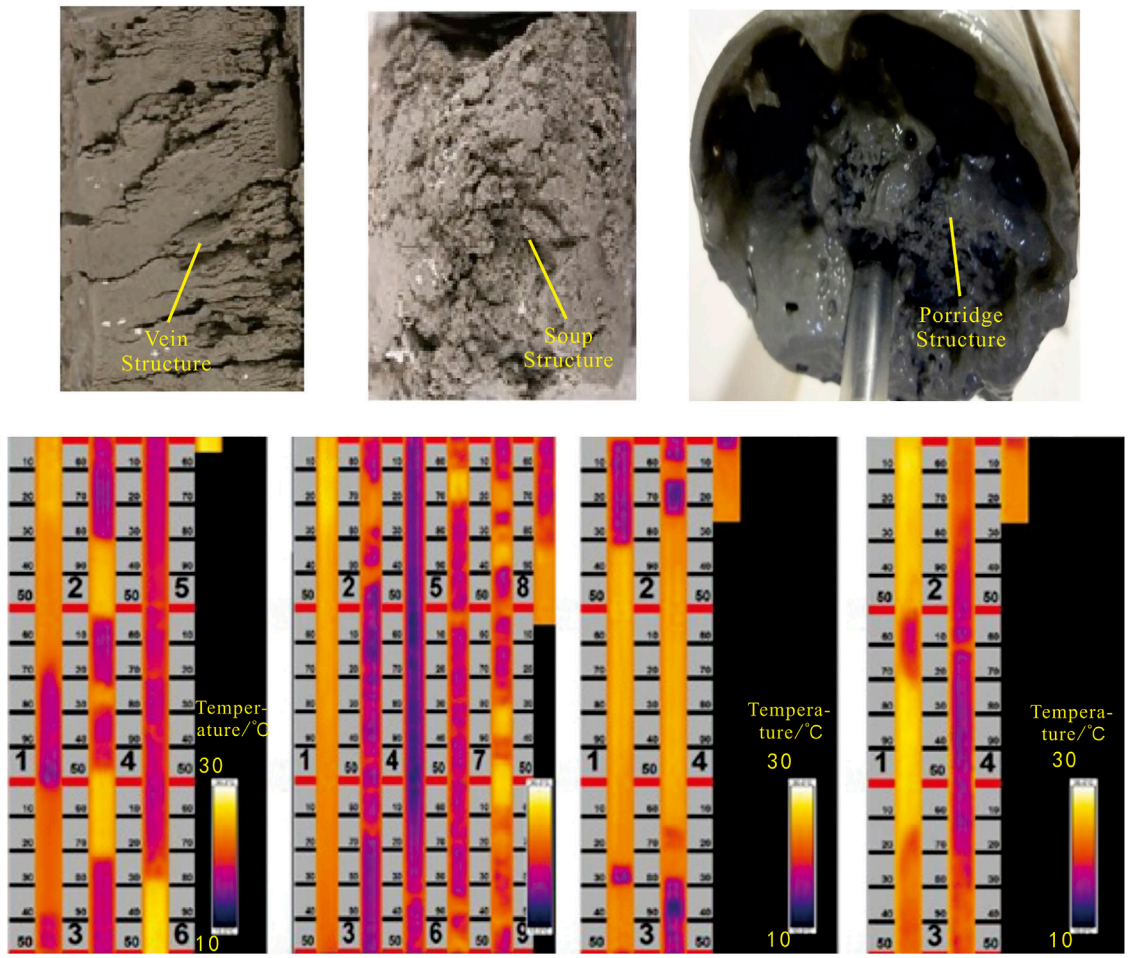

FIGURE 2 | Characteristics of gas hydrates and gas hydrate-bearing sediments at site W17 based on drilling cores and infrared scanning images.

concentrations of ethane and propane were detected in the fractured gas (gas extracted from the core expansion fracture) and pressure release gas in the pressure cores from sites W17 and W19 (**Figure 4**).

The $C_1/(C_2+C_3)$ value for the fissure gas and air release slowly decreases with increasing depth in site W17, and the $C_1/(C_2+C_3)$ values are around 800 (**Figure 4A**). At the top of the bottom interface of the gas hydrate reservoir, the values exhibit mutation at around 206 m. The $C_1/(C_2+C_3)$ values of the gas samples from the hydrate reservoir are less than 300, and the ethane and propane contents slowly increase with increasing depth. In addition, mutations occur near 206 m at the top of the bottom interface of the gas hydrate reservoir, and the concentration is more than 104 ppm, which is higher than the ethane and propane contents. Presumably, the gas source of the hydrates is mainly a mixture of thermogenic gas (thermal) and microbial gas. The decrease of propane content below 206 m may the result of lateral gas migration and accumulation near 206 m to form gas hydrate. An abrupt change in the $C_1/(C_2+C_3)$ values was observed at the top of the hydrate reservoir interface in site W19 (**Figure 4B**), the $C_1/(C_2+C_3)$ values within the reservoir decreased with increasing depth, the $C_1/(C_2+C_3)$ values of the gas samples from the hydrate reservoir are less than 300, and the propane content is higher than the ethane content near the top boundary of the gas hydrate reservoir. It is speculated that the gas hydrate reservoir in site W19 was mainly formed from a mixture of thermogenic gas and microbial gas. In addition, the carbon isotope compositions of the methane gas from sites W17 and W19 are −45‰ to −80‰, and the methane/ethane ratio is 90–1000; this further indicates that the gas source is mainly a mixture of thermogenic gas and microbial gas (**Figure 5**).

Logging Characteristics of Gas Hydrates

Gas hydrate reservoirs can be identified by analyzing the logging characteristics of the sedimentary strata. The distribution of the gas hydrates in the sedimentary layer can be estimated effectively using the multi-means exploration technology of geophysical logging (Lu et al., 2008; Liang et al., 2010; Liang et al., 2017a). The gas hydrate reservoirs with different types or different saturations have different logging responses: the resistivity and acoustic velocity in gas hydrate reservoirs are significantly higher than those of the surrounding sediments, while the neutron porosity, density, and natural gamma are slightly lower, and the acoustic velocity, density, and neutron

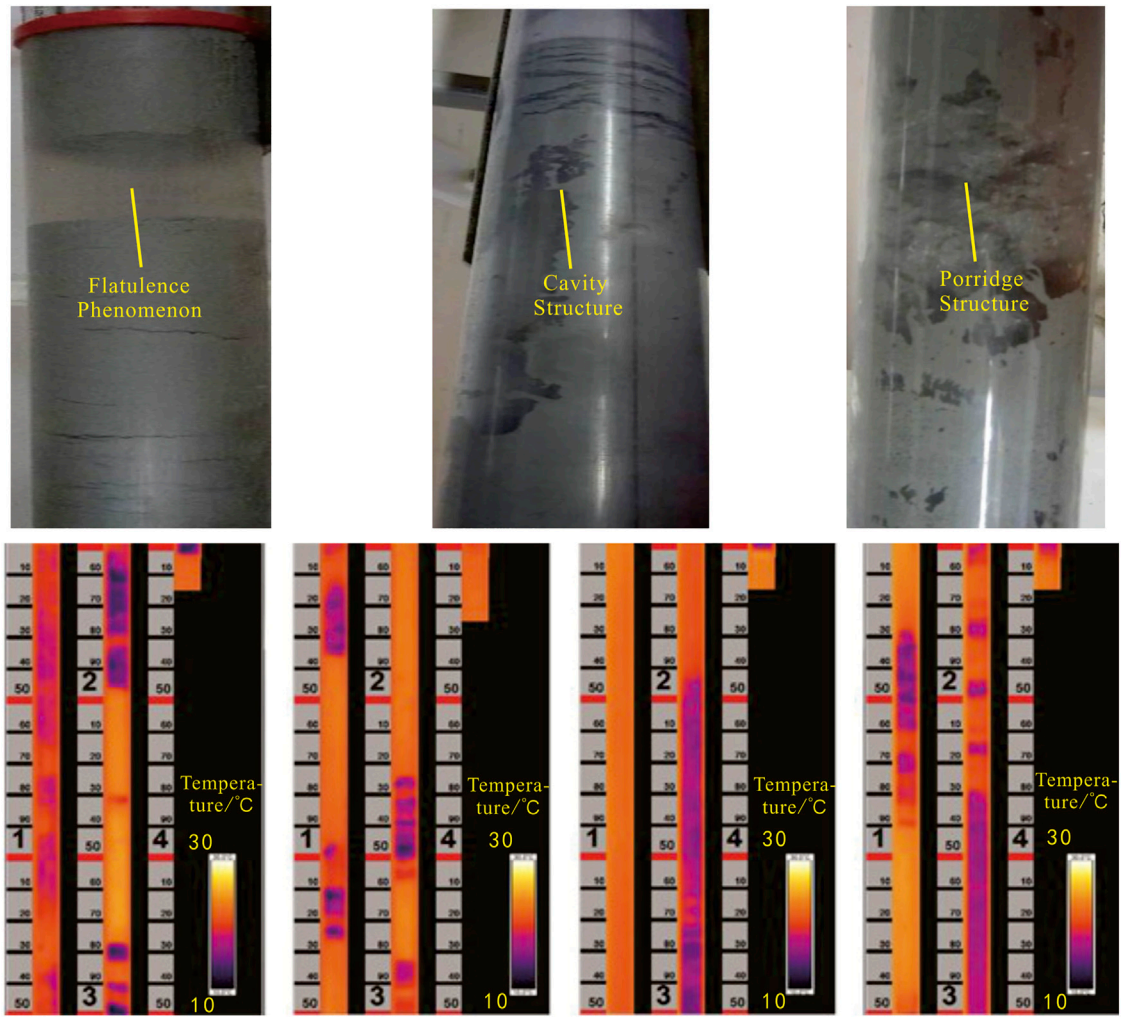

FIGURE 3 | Characteristics of gas hydrates and gas hydrate-bearing sediments at site W19 based on drilling cores and infrared scanning images (Zhang et al., 2017).

porosity are significantly lower (Wang et al., 2003; Mo et al., 2008; Liang et al., 2017b).

Site W17 is located in the southeastern part of the study area, at the bottom of the northern continental slope of the South China Sea, with a water depth of 1249 m and a maximum well depth of 319 m. The logging curve for site W17 shows that the abnormal characteristics of "two highs and three lows" values of the logging curves are obvious in the 1460–1522 m section (**Figure 6**). The acoustic velocity increases rapidly from 1460 m to 1522 m and reaches the highest value of 2295 m s^{-1} at 1490 m. The upper part of the density curve is relatively gentle, with little change. The lower part is the 1510–1522 m section, in which the lowest density is 1.72 g cm^{-3}. The resistivity curve starts at 1460 m and changes in a wavy shape with increasing depth. It also exhibits the abnormal features of low values at both ends and large values in the middle. The maximum resistivity value is 4.6 Ω m. The neutron porosity decreases due to the filling of the sediment pores with hydrates and/or free gas. The porosity curve begins to decrease slowly at 1460 m, with a minimum porosity value of 28%. The natural gamma logging curve is relatively flat overall, and there is no large mutation. It is concluded that the deposition near site W17 is relatively stable, and the grain size of the hydrate enrichment section is mainly medium silt to coarse silt (Liang et al., 2009; Guo et al., 2017; Yang et al., 2020). Obvious turbidity deposits are observed in this section of the channel on the seismic profile beside the well, which is speculated to be the levee facies of the turbidity current. The overall seismic signal is relatively continuous, and the strongly reflective hydrate-bearing sediment layer is located near the natural levee (**Figure 7**). According to the logging curve for site W17, it is speculated that there is a ~ 45 m thick hydrate sedimentary layer near the site, with the average saturation of 19.4%, and an ~ 12 m thick free gas layer beneath the hydrate layer, with the average saturation of 30.1%.

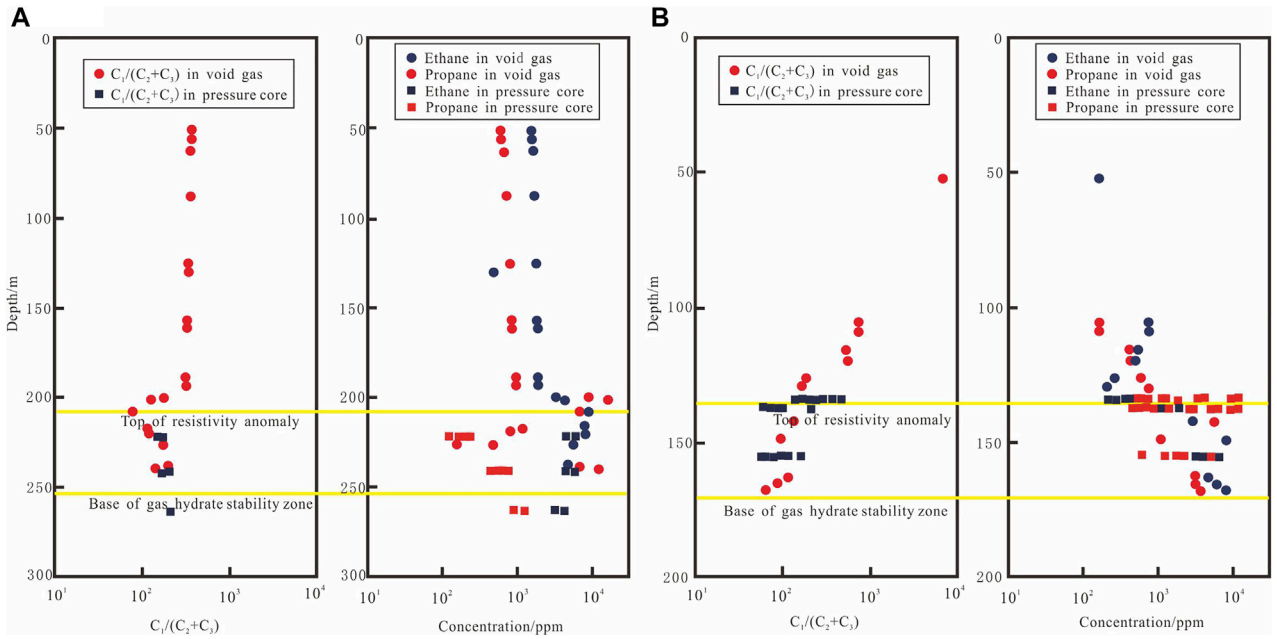

FIGURE 4 | Vertical variations in the gas compositions in sites W17 and W19.

Site W19 is located in the central and southern parts of the study area, and it is also at the bottom of the continental slope, with a water depth of 1274 m and a maximum well depth of 245 m. The logging anomaly at site W19 mainly shows that the acoustic velocity increases rapidly from 1788 m·s^{-1} from 1411 m–1432 m (**Figure 8**). It rapidly reaches 2522 m s^{-1}, and the highest value is 2790 m s^{-1}.

Then, it drops sharply to 1821 m s^{-1} at 1432 m. The acoustic velocity curve oscillates and decreases with increasing depth. The entire section of the density curve is relatively flat with little change, and there is no low segment that corresponds to the acoustic velocity curve. Therefore, it is speculated that the hydrates occur in the form of diffuse hydrates, and there is no obvious free gas layer under the hydrate-bearing sedimentary layer. The resistivity rises rapidly from 1 Ω m to 8 Ω m starting at 1411 m. The maximum value (8.67 Ω m) occurs at 1415 m, and then, it oscillates with increasing depth. The neutron porosity decreases due to the filling of the sediment pores with hydrates, and the minimum porosity value is 26%. The natural gamma logging curve decreases slightly in the hydrate formation (**Figure 7**), the effective thickness of gas hydrate layer is about 25 m and the average saturation is 30.4%. According to the core characteristics, there are three hydrate enrichment layers in site W19. The gas hydrates in the 1401–1403 m are mainly in fine silts and silts with relatively coarse grain size, and there are silts and muds interlayers with vertical discontinuity. Based on the seismic reflection characteristics, it can be concluded that the hydrates in this section are concentrated in the shallow natural gas layer of the slump body. In the 1412–1425 m and 1430–1438 m intervals, the granularity of the hydrate layer is low, the vertical continuity is good. It is a powdery sand-shale deposit, with a soup-like core structure and fracture development (**Figure 9**). For the hydrate layer with the relatively cluttered seismic reflection, it is speculated that the hydrate development channel is located in the slump. The hydrate layer with a wedge seismic reflection is most likely a silty turbidity deposit such as levee facies.

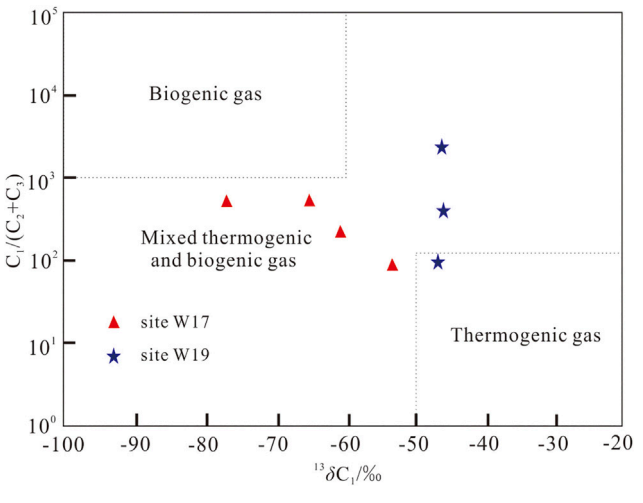

FIGURE 5 | Cross plot of methane carbon isotope ($\delta^{13}C_1$) and $C_1/(C_2+C_3)$ of gas hydrates.

Seismic Reflection and Gas Migration Characteristics of Hydrate Layer

The seismic exploration of the hydrates in the study area revealed that the bottom-simulating reflector is an important indicator of the hydrate content of the sedimentary strata (Santamarina et al., 2015;

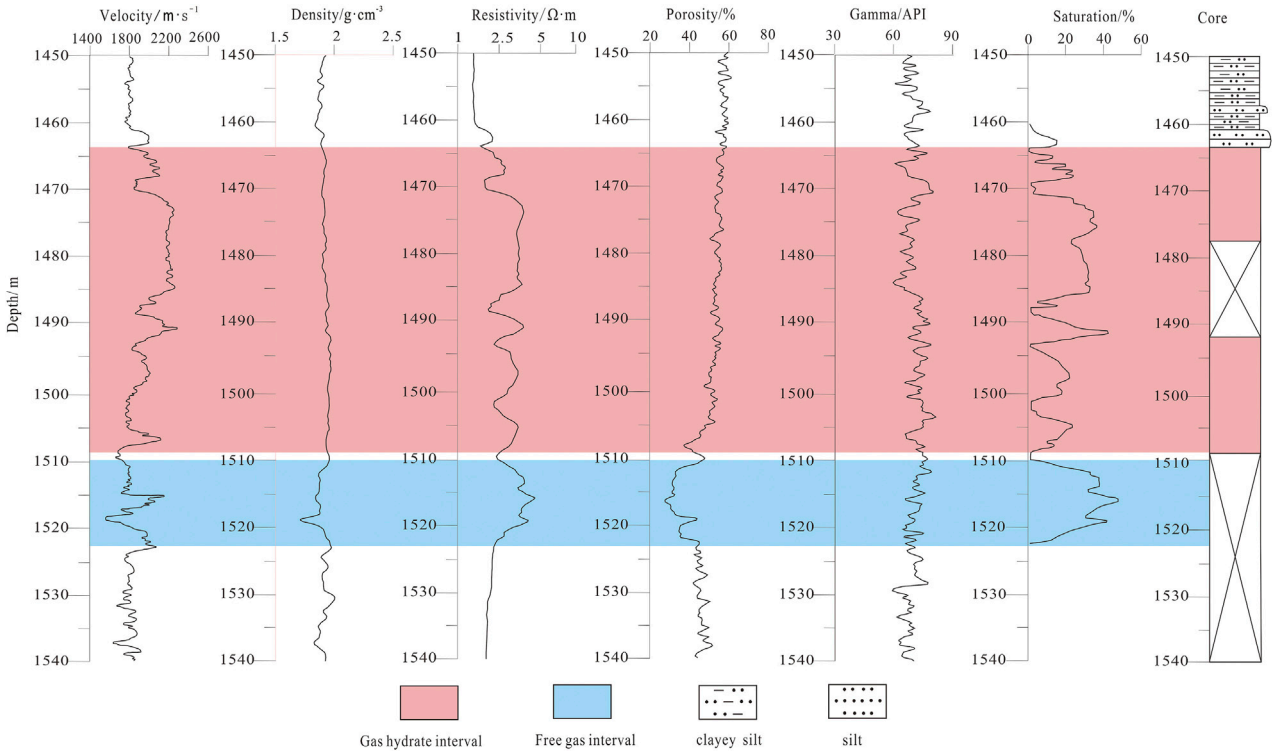

FIGURE 6 | Characteristics of well logging curves and lithology of site W17.

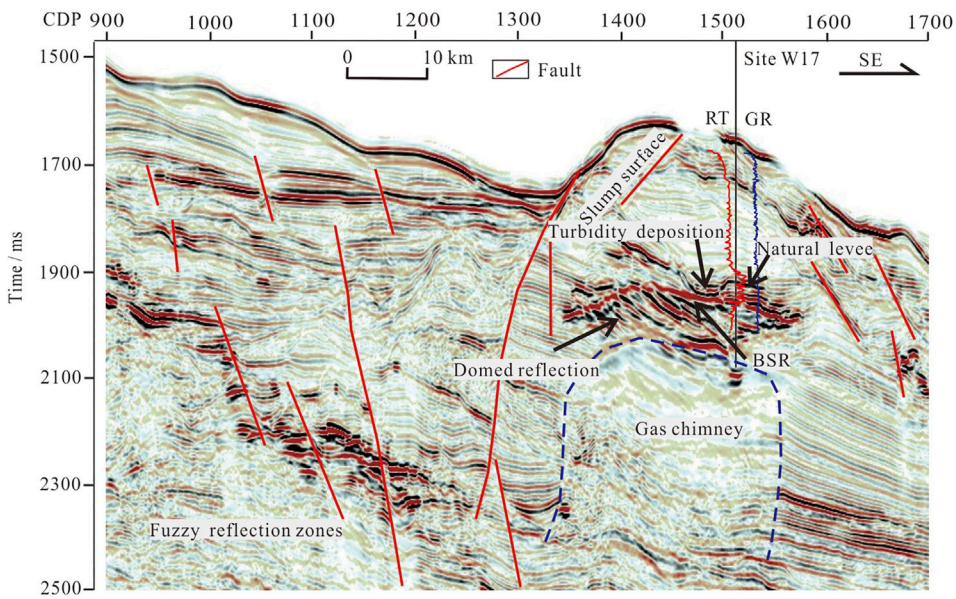

FIGURE 7 | The seismic reflection profile across site W17. The location of the seismic profile is shown in **Figure 1B**.

Sua et al., 2018; Shukla et al., 2019). It usually has a medium-strong amplitude and medium-high continuous reflection on the seismic profile, which is roughly parallel to the seafloor reflection. The BSR is usually oblique to the formation in the slope zone. If there is free gas in the formation, due to the large wave impedance difference between the hydrates and free gas, the seismic reflection is enhanced and an

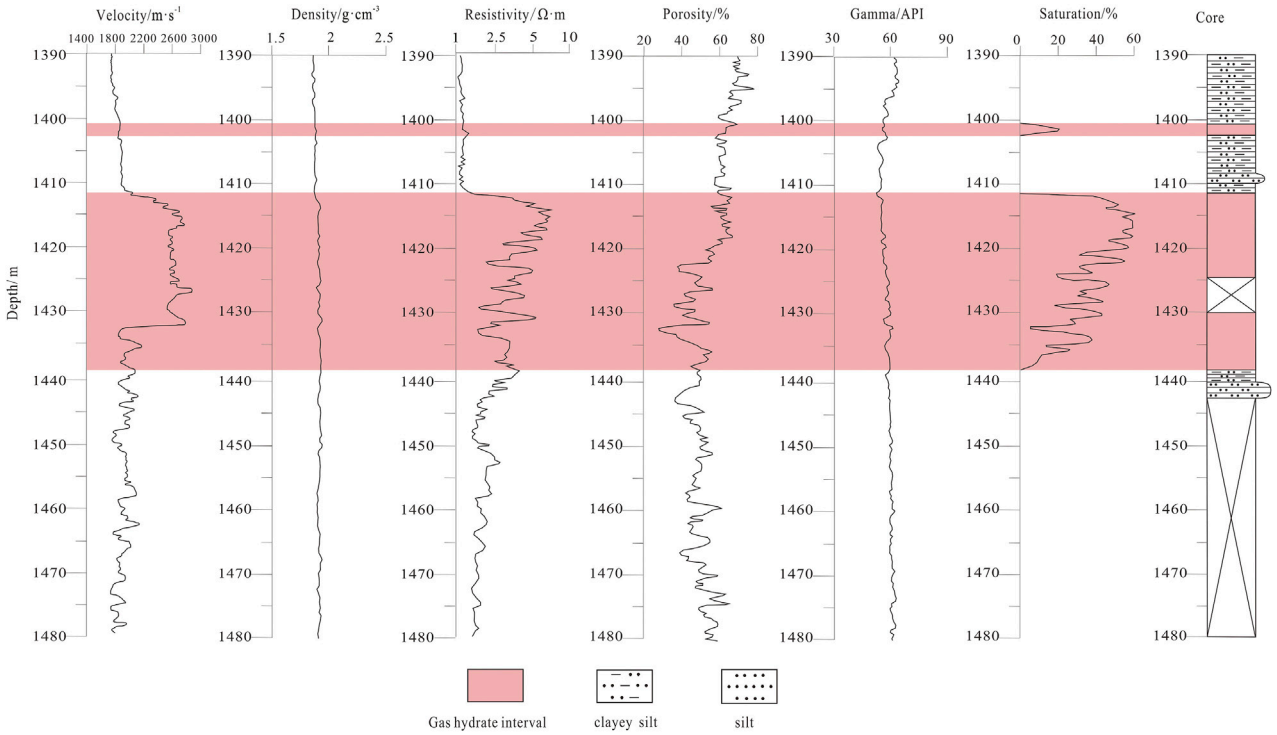

FIGURE 8 | Characteristics of well logging curves and lithology of site W19.

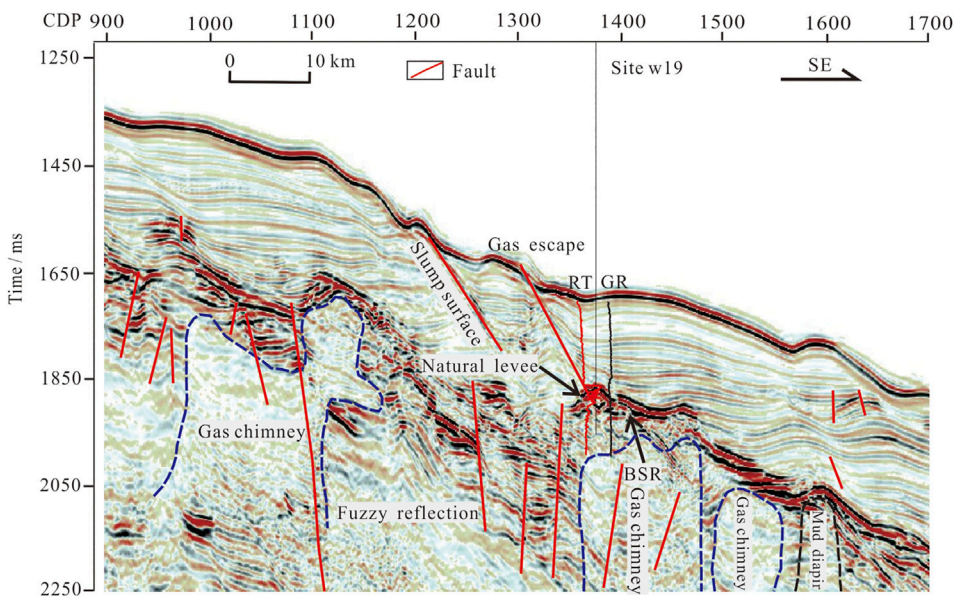

FIGURE 9 | The seismic reflection profile across site W19. The location of the seismic profile is shown in **Figure 1B**.

amplitude enhancer is formed (Su et al., 2014; Yang et al., 2017b; Zhang et al., 2020). The seismic wave velocity of the hydrate-bearing sedimentary layer is relatively high, so the reflection time is short, and the seismic event on the profile stretches upward; while the seismic wave velocity of the free gas-bearing stratum is relatively low and the reflection time is short, which causes downward stretching of the seismic event, forming an abnormal eyeball velocity amplitude structure (V'AMP). In addition, when the sedimentary formation

is filled with hydrates and is further cemented, the formation's pore space becomes uniform, and the seismic profile shows blank or weak amplitude zones. The waveform of the BSR subwave generally has a negative polarity, which is opposite to the waveform of the wave reflected by the seafloor, and the absolute value of the reflection coefficient is relatively large. These seismic reflection characteristics of hydrates can be used to identify the existence of hydrate-bearing deposits.

The BSR in the seismic profile cross site W17 has a medium-strong amplitude and medium-high continuity (**Figure 8**). There is an obvious amplitude gap above the BSR, and the formation had good ductility. The polarity of the BSR waveform is opposite to that of the submarine waveform. Under the temperature and pressure conditions, the BSR waveform cuts through the seismic event of the formation, and the seismic event exhibits an enhanced reflection, which has quite obvious BSR characteristics. An obvious domed reflection occurs below the BSR, this is due to the velocity amplitude anomaly augen structure, which is formed by the hydrates in the stable zone, with the upper interface causing the seismic reflection wave velocity to increase and the reflection time to shorten. On the seismic profiles, the seismic event bends upward, and the seismic wave velocity is lower due to the low amount of free gas, producing a prolonged reflection time under the gas hydrate stable zone. On the seismic profiles, the seismic event bending exhibits an obvious V'AMP phenomenon. The shallow deposits above the BSR are mound and sheet slump deposits, and the entire deposit is composed of mounds and sheets. The seismic event in the sedimentary layer exhibits an asymmetric wavy reflection structure and gradually migrates upward towards the continental slope. The high wave impedance (RT) value corresponds to the hydrate layer in the natural levee, and the gamma ray (RT) curve does not change much. The cap layer is developed above the BSR, a fracture pathway exists at the edge of the hydrate layer, and gas escapes to the seabed through this pathway. The reinforced reflection is obvious below the BSR, there is a lot of free gas, and the fault structure is developed below the BSR. There are large gas chimneys and many disorderly and fuzzy reflections on the seismic profile.

The BSR on the seismic profiles cross site W19 exhibits enhanced reflection, with the polar opposite to the bottom reflection polarity (**Figure 9**). The high wave impedance (RT) value corresponds to the gas hydrate layer in the natural embankment, while the low gamma ray value corresponds to the gas hydrate layer. On the seismic profile, the fractures are well developed on the left side of the BSR, and many disorderly and fuzzy reflections can be seen below the BSR, indicating that a large number of gas chimneys exist near site W19. The shallow deposits above the BSR are sheet-like and U-shaped slump deposits (Wu et al., 2003, Wu et al., 2007). Their overall distribution is sheet-like, and an obvious slip surface at the bottom of the slump deposit and erosion trough deposits above the BSR exist. The erosion trough deposits exhibit high frequency, medium amplitude, and U-shaped filling features on seismic reflection (**Figure 9**). In addition, faults that extending to the seafloor indicate gas escaping. The seismic profile below the BSR exhibits a medium frequency and medium amplitude, which is interpretated as submarine fan deposits in the upper Miocene.

Through many years of seismic and geological investigation and oil and gas exploitation in the Pearl River Mouth Basin, it has been shown that there are many natural gas fields in the Shenhu Sea area in the southern part of the basin, especially in the Baiyun sag, in which the natural gas distribution area is concentrated. That is, there is plenty of hydrocarbon gas in the deep layer near the study area. Under the effect of the formation pressure, the deep gas gradually migrates upward along the gas chimneys, unconformity surfaces, faults, fractures, and sandstone channels, and then, it gathers in the hydrate stability zone, which has suitable temperature and pressure conditions. There are several vertical fuzzy zones on the seismic reflection profile in the deep and central parts of the study area. These phenomena are gas chimneys formed by the movement of deep gas upward along the fractures, causing disturbance of the stratum. In addition, submarine canyon channel is an important migration pathway of terrigenous materials to the deep sea, and the formation and development of turbidity channels and levees are closely related to gas hydrate accumulation (Kuang et al., 2018). Channel-filling sediments is not only a good reservoir, but also a good gas migration and transport pathway, which is a dominant gathering place for gas hydrate formation and occurrence (Kuang and Guo, 2011; Davies et al., 2012).

Gas chimneys and fault structures are well developed near site W17, and there are gas chimneys under the BSR (**Figure 8**). Gas chimneys and deep faults are developed. The hydrocarbon gases in the middle and deep strata migrated to the seafloor along the dense fractures and faults and formed a hydrate layer with a high saturation under the low temperature and pressure conditions. There are also faults and gas chimney clusters near site W19, which are larger in scale than those at site W17 (**Figure 9**). Thermogenic gas migrates upward with the overpressure fluid through deep and large faults, and then, it migrates laterally along the conformable surfaces with appropriate porosity and permeability to form reservoirs in suitable stratigraphic traps and/or structures. Under the action of the fluid potential, part of the thermogenic gas continues to migrate into the shallow strata along the channels formed by the faults and fractures. Once the temperature and pressure conditions of the hydrocarbon gas in the fracture channels are suitable, a seepage hydrate is formed. In addition, the microbial gas in the shallow strata can migrate and accumulate through sediment pores or interlayer micro-fissures to form diffusive hydrates, and the microbial gas in the lower part of the gas hydrate stable zone can also migrate upward through gas chimneys, mud diapirs, and faults to form gas hydrates.

DISCUSSION

How is Gas Hydrate Production Test Site Selected?

The above analysis shows that gas hydrates in sites W17 and W19 belong to diffuse type. The reservoir properties of two sites show

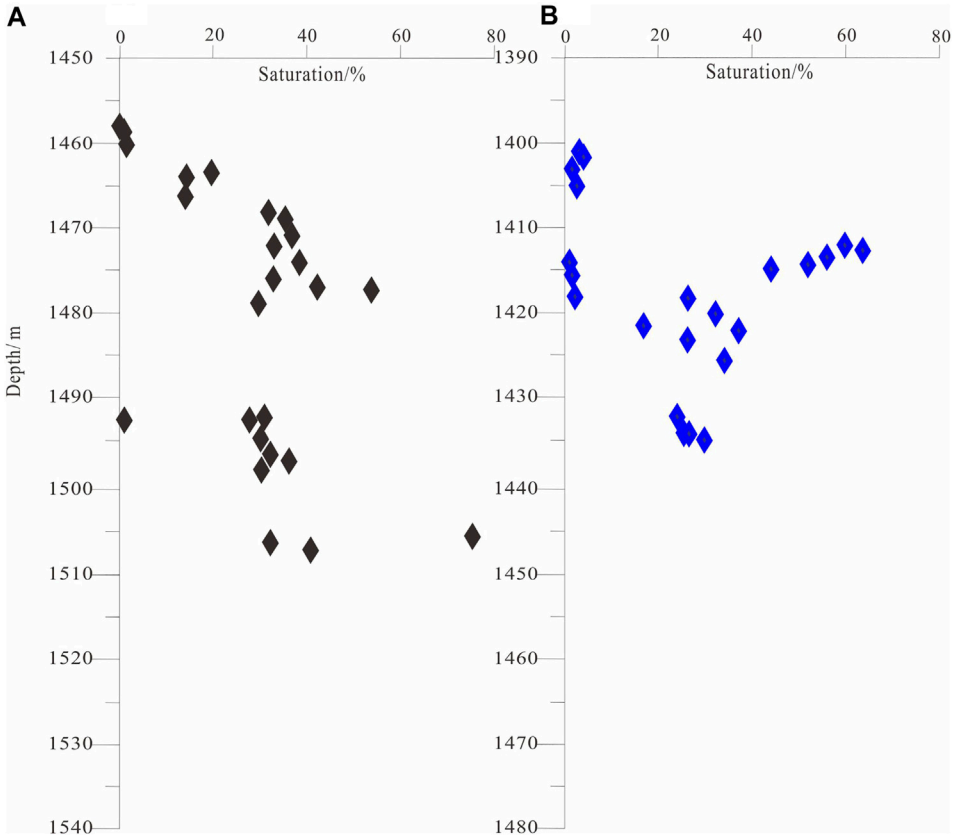

FIGURE 10 | Vertical variations in the gas hydrate saturation in sites W17 and W19.

similar permeability, porosities, and shale contents. The engineering geological conditions (e.g., water depth, bottom slope, reservoir depth, and engineering mechanics) conform to the conditions for gas hydrate exploration. The following questions are thus raised: why was site W17 chosen as the final test site rather than site W19? The reservoir saturation, reservoir thickness, and gas sealing ability of these two sites are analyzed and discussed below.The gas hydrate saturation was calculated from the desalination degree of the chloride ions in the pore water of the hydrate-bearing deposits from sites W17 and W19 (**Figure 10**). At site W17, the thickness of the gas hydrate-bearing sediment layer is about 45 m, and the maximum saturation is 76%, with an average of 33%. At site W19, the thickness of the gas hydrate-bearing sediment layer is about 25 m, and the maximum saturation is 68%, with an average of 31%. Through the seismic profile analysis and well logging curve calculation, the gas hydrate sediments in W17 site containing thicker, and higher saturation of gas hydrate, the W17 orebody area is 3 times than that of W19 orebody, and the resources of W17 orebody is 7 times higher than that of in W19 site. Beside the W17 orebody has good continuity reservoir, sealing layer, fault pathway at orebody edge. The logging curve shows that the thickness of the gas layer is 12 m and the average gas saturation is 30.1%, which can provide sufficient gas source for gas hydrate formation. The seismic profile shows that there is a large gas chimney structure under the gas layer, which is the upward migration channel of deep cracked gas and the gas source guarantee for the formation of free gas layer. While site W19 has thinner gas hydrate reservoirs, faults directly leading to the bottom of the seafloor above the BSR, and gas escape. Thus, site W17 was chosen for the hydrate exploration.

Why do Silty Clay Sediments Develop High Saturation of gas Hydrates?

The gas hydrates in the study area are mainly developed in or near the levee facies sediments. In this study, it was revealed that the sand-bearing sediments in the levee facies are relatively developed, and the sandy reservoir is a good sedimentary environment for gas hydrate formation (Riedel et al., 2011; Crutchley et al., 2017). Compared with muddy and silty mudstone sediments, the sandy sediments in the levee facies have more reservoir space due to their higher porosity and permeability (Su et al., 2018; Liang et al., 2019; Meng et al., 2021). Hydrocarbon gases tend to accumulate in strata with high porosities and permeabilities, which are more conducive to the formation of gas hydrates with higher saturation (Lu et al., 2011; Dai et al., 2012; Bahk et al., 2013). The core samples from sites W17 and W19 in the study area indicate that the hydrate deposits are fine-grained silty clay deposits. However, the highest gas

hydrate saturation at site W17 is 76%, with an average of 33%; while the highest gas hydrate saturation at site W19 is 68%, with an average of 31%. Both of these sites have high saturation. The gas hydrates in the study area are diffused within the fine-grained sediments, and it is difficult to form high saturation gas hydrates through diffusion migration alone because the capillaries with a high resistance need to be broken through before fluid migration can occur. Therefore, what caused the high saturation in the fine-grained silty clay sediments? Some studies have reported that the gas mainly reaches the gas hydrate stable zone via diffusion migration, water-soluble migration, and free migration through certain migration and transport channels (Collett et al., 2009). Post-drilling research in the study area revealed that the migration and transport pathways, such as gas chimneys, mud diapers, and faults, which play a key role in the accumulation of high saturation gas hydrates (Wang et al., 2014; Su et al., 2017). Gas chimneys and mud diapirs are identified in the lower part of the BSR, and faults are developed nearby, which should be the migration channel through which the deep gas-bearing fluid migrates into the gas hydrate stable zone. In addition, the study area is located close to the center of Baiyun Sag, and thermogenic gas from the deep part of the sag continuously migrates upward through the faults, diapirs, and gas chimneys, and then, it mixes with microbial gas. These mixed gases then migrate into the hydrate stable zone to form high saturation gas hydrates (Zhang et al., 2017).

CONCLUSION

Based on logging data, seismic data, drilling core data, gas composition and carbon isotope characteristics, and gas hydrate saturation data, the logging and geophysical characteristics and variations in the gas hydrate-bearing sediments were summarized.

1) the gas hydrates are diffusion type, with reservoirs dominated by clayey silt sediments, and the gas hydrate-bearing layers are characterized by soup-like, porridge-like, cavity, and vein structures;
2) the resistivity and acoustic velocity of gas hydrate formation are significantly higher than those of the surrounding sediments, while the neutron porosity, density, and natural gamma are slightly lower; the Bottom Simulating Reflectors (BSRs) in seismic profiles exhibit the exist of gas hydrates;
3) gas chimneys and faults are well-developed beneath the BSRs, and hydrocarbon gases can easily migrate into the gas hydrate reservoirs in areas with stable temperature and pressure conditions;
4) the gas hydrate saturation is high, the highest saturation in site W17 was up to 76%, with an average of 33%; while the highest saturation in site W19 was up to 68%, with an average of 31%. The gas source is considered as mixed gas of thermogenic gas and microbial gas.

By comparing the core samples and geophysical characteristics of sites W17 and W19 in the study area and calculating the thickness, distribution area, and saturation of the gas hydrate deposition layer, it was found that site W17 is characterized by a thick layer, large area, high saturation, and good sealing, besides, the gas sources are sufficient and gas migration pathway are well developed, thus site W17 was established as the test production site. The development of gas chimney and faults provides driving force for the upward migration of deep gas, and the gas migrates to gas hydrate stable zone in forms of diffusion, water soluble and free state, forming high saturation of diffusion gas hydrates.

DATA AVAILABILITY STATEMENT

The original contributions presented in the study are included in the article/Supplementary Material, further inquiries can be directed to the corresponding author.

AUTHOR CONTRIBUTIONS

JL: Investigation, Formal analysis, Writing—original draft. MM: Review and editing. JL: Supervision. JR: Supervision in Geology. YH: Investigation and seismic analysis. TL: Logging analysis. MX: Geophysical interpretation. XW: Figure drawing.

FUNDING

This work was supported by Key Special Project for Introduced Talents Team of Southern Marine Science and Engineering Guangdong Laboratory (Guangzhou) (No. GML2019ZD0105), Guangdong Province Marine Economic Development (Six Major Marine Industries) Special Fund Project (No. [2021] No. 58), and the National Natural Science Foundation of China (No. 42102144). the Geological Survey Project of China (No. DD20221705, No. DD20221700).

ACKNOWLEDGMENTS

Thank to those who contributed to the success of the China National Gas Hydrate Program Expeditions 3 (GMGS3). Editor Jinan Guan and two reviewers that provide constructive suggestions are gratefully appreciated. We also thank LetPub for its linguistic assistance during the preparation of this manuscript.

REFERENCES

Bahk, J.-J., Kim, D.-H., Chun, J.-H., Son, B.-K., Kim, J.-H., Ryu, B.-J., et al. (2013). Gas Hydrate Occurrences and Their Relation to Host Sediment Properties: Results from Second Ulleung Basin Gas Hydrate Drilling Expedition, East Sea. *Mar. Petroleum Geol.* 47, 21–29. doi:10.1016/j.marpetgeo.2013.05.006

Booth, J. S., Winters, W. J., and Dillon, W. P. (1994). Circumstantial Evidence of Gas Hydrate and Slope Failure Associations on the United States Atlantic Continental Margin. *Ann. N. Y. Acad. Sci.* 715 (1), 487–489. doi:10.1111/j.1749-6632.1994.tb38863.x

Boswell, R., Frye, M., Shelander, D., Shedd, W., McConnell, D. R., and Cook, A. (2012). Architecture of Gas-Hydrate-Bearing Sands from Walker Ridge 313, Green Canyon 955, and Alaminos Canyon 21: Northern Deepwater Gulf of Mexico. *Mar. Petroleum Geol.* 34 (1), 134–149. doi:10.1016/j.marpetgeo.2011.08.010

Chen, D. F., Chen, X. P., and Chen, G. Q. (2002). Geology and Geochemistry of Cold Seepage and Venting-Elated Carbonates. *Acta Sedimentol. Sin.* 20 (1), 34–40. (In Chinese with English abstract). doi:10.3969/j.issn.1000-0550.2002.01.007

Chong, Z. R., Yang, S. H. B., Babu, P., Linga, P., and Li, X.-S. (2016). Review of Natural Gas Hydrates as an Energy Resource: Prospects and Challenges. *Appl. Energy* 162, 1633–1652. doi:10.1016/j.apenergy.2014.12.061

Collett, T. S. (2002). Energy Resource Potential of Natural Gas Hydrates. *AAPG Bull.* 86 (11), 1971–1992. doi:10.1306/61eeddd2-173e-11d7-8645000102c1865d

Collett, T. S., Johnson, A. H., Knapp, C. C., and Boswell, R. (2009). American Association of Petroleum Geologists Memoir, Natural Gas Hydrates. *A Rev.* 89, 146–219.

Collett, T. S. (2010). Resource Potential of Gas Hydrates: Recent Contributions from International Research and Development Projects. *Pet. Geol. Conf. Ser.* 7, 1151–1154. doi:10.1144/0071151

Crutchley, G. J., Kroeger, K. F., Pecher, I. A., Mountjoy, J. J., and Gorman, A. R. (2017). Gas Hydrate Formation amid Submarine Canyon Incision: Investigations from new Zealand's Hikurangi Subduction Margin. *Geochem. Geophys. Geosyst.* 18, 4299–4316. doi:10.1002/2017gc007021

Dai, S., Santamarina, J. C., Waite, W. F., and Kneafsey, T. J. (2012). Hydrate Morphology: Physical Properties of Sands with Patchy Hydrate Saturation. *J. Geophys. Res. Solid Earth* 117, B11205. doi:10.1029/2012jb009667

Davies, R. J., Thatcher, K. E., Mathias, S. A., and Yang, J. (2012). Deepwater Canyons: An Escape Route for Methane Sealed by Methane Hydrate. *Earth Planet. Sci. Lett.* 323, 72–78. doi:10.1016/j.epsl.2011.11.007

Demirbas, A. (2010). Methane Hydrates as Potential Energy Resource: Part 2 - Methane Production Processes from Gas Hydrates. *Energy Convers. Manag.* 51 (7), 1562–1571. doi:10.1016/j.enconman.2010.02.014

Fang, Y., Wei, J. G., Wei, J., Lu, H., Liang, J., Lu, J. a., et al. (2019). Chemical and Structural Characteristics of Gas Hydrates from the Haima Cold Seeps in the Qiongdongnan Basin of the South China Sea. *J. Asian Earth Sci.* 182, 103924. doi:10.1016/j.jseaes.2019.103924

Fu, N., Lin, Q., and Liu, Y. L. (2011). Analysis on Potential Gas Source of Gas Hydrate from the Original Characteristics of Shallow Gas in the North of the South China Sea. *Geoscience* 25 (2), 332–339. (In Chinese with English abstract). doi:10.3969/j.issn.1000-8527.2011.02.017

Guo, Y. Q., Yang, S. X., Liang, J. Q., Lu, J. A., Lin, L., and Kuang, Z. G. (2017). Characteristics of High Gas Hydrate Distribution in the Shenhu Area, Northern Slope of South China Sea. *Earth Sci. Front.* 24 (4), 24–31. (In Chinese with English abstract). doi:10.13745/j.esf.yx.2016-12-28

He, J. X., Yan, W., Zhu, Y. H., Zhang, W., Gong, F., Liu, S. L., et al. (2013). Biogenetic and Sub-biogenetic Gas Resource Potential and Genetic Types of Natural Gas Hydrate in the Northern Marginal Basins of the South China Sea. *Nat. Gas. Ind.* 33 (6), 121–134. (In Chinese with English abstract). doi:10.3787/j.issn.1000-0976.2013.06.023

He, J. X., Yao, Y. J., Liu, H. L., and Wan, Z. F. (2008). Genetic Types of Natural Gas and Characteristic of the Gas Source Composition in Marginal Basins of the Northern South China Sea. *Geol. China* 35 (5), 1007–1016. (In Chinese with English abstract). doi:10.3969/j.issn.1000-3657.2008.05.020

He, Y., Zhong, G., Wang, L., and Kuang, Z. (2014). Characteristics and Occurrence of Submarine Canyon-Associated Landslides in the Middle of the Northern Continental Slope, South China Sea. *Mar. Petroleum Geol.* 57, 546–560. doi:10.1016/j.marpetgeo.2014.07.003

Hyndman, R. D., and Davis, E. E. (1992). A Mechanism for the Formation of Methane Hydrate and Seafloor Bottom-Simulating Reflectors by Vertical Fluid Expulsion. *J. Geophys. Res.* 97 (B5), 7025–7041. doi:10.1029/91jb03061

Jin, J., Wang, X., He, M., Li, J., Yan, C., Li, Y., et al. (2020). Downward Shift of Gas Hydrate Stability Zone Due to Seafloor Erosion in the Eastern Dongsha Island, South China Sea. *J. Ocean. Limnol.* 38, 1188–1200. doi:10.1007/s00343-020-0064-z

Kawasaki, T., Ukita, T., Fujii, T., Noguchi, S., and Ripmeester, J. A. (2011). Particle Size Effect on the Saturation of Methane Hydrate in Sediments - Constrained from Experimental Results. *Mar. Petroleum Geol.* 28 (10), 1801–1805. doi:10.1016/j.marpetgeo.2010.11.007

Klauda, J. B., and Sandler, S. I. (2005). Global Distribution of Methane Hydrate in Ocean Sediment. *Energy fuels.* 19 (2), 459–470. doi:10.1021/ef049798o

Kuang, Z. G., Fang, Y. X., Liang, J. Q., Lu, J. A., and Wang, L. (2018). Geomorphological-geological-geophysical Signatures of High-Flux Fluid Flows in the Eastern Pearl River Mouth Basin and Effects on Gas Hydrate Accumulation. *Sci. China (Earth Sci.* 61 (7), 914–924.

Kuang, Z. G., and Guo, Y. (2011). The Sedimentary Facies and Gas Hydrate Accumulation Models since Neogene of Shenhu Area, Northern South China Sea. *Earth Sci. — J. China Univ. Geosciences* 36 (5), 914–920. (In Chinese with English abstract). doi:10.3799/dqkx.2011.096

Kvenvolden, K. A. (1993). Gas Hydrates-Geological Perspective and Global Change. *Rev. Geophys.* 31 (2), 173–187. doi:10.1029/93rg00268

Kvenvolden, K. A., and Lorenson, T. D. (2001). The Global Occurrence of Natural Gas Hydrate. *Nat. Gas Hydrates Occur. Distribution, Detect.* 124, 3–18.

Lee, M. W., and Collett, T. S. (2012). Pore- and Fracture-Filling Gas Hydrate Reservoirs in the Gulf of Mexico Gas Hydrate Joint Industry Project Leg II Green Canyon 955 H Well. *Mar. Petroleum Geol.* 34, 62–71. doi:10.1016/j.marpetgeo.2011.08.002

Lee, M. W., Hutchinson, D. R., Dillon, W. P., Miller, J. J., Agena, W. F., and Swift, B. A. (1993). Method of Estimating the Amount of *In Situ* Gas Hydrates in Deep Marine Sediments. *Mar. Petroleum Geol.* 10 (5), 493–506. doi:10.1016/0264-8172(93)90050-3

Liang, J. Q., Wang, H. B., Su, X., Fu, S. Y., Wang, L. F., Guo, Y. Q., et al. (2014). Natural Gas Hydrate Formation Conditions and the Associated Controlling Factors in the Northern Slope of the South China Sea. *Nat. Gas. Ind.* 2 34 (7), 128–135. (In Chinese with English abstract). doi:10.3787/j.issn.1000-0976.2014.07.022

Liang, J. Q., Zhang, G. X., Lu, J. A., et al. (2016). Accumulation Characteristics and Genetic Models of Natural Gas Hydrate Reservoirs in the NE Slope of the South China Sea. *Nat. Gas. Ind.* 36 (10), 157–162. (In Chinese with English abstract). doi:10.3787/j.issn.1000-0976.2016.10.020

Liang, J., Wang, M. J., and Guo, Y. Q. (2006). Studies of Seismic Velocity about Gas Hydrate in North Slope of the South China Sea. *Geoscience* 20 (1), 123–129. (In Chinese with English abstract). doi:10.1007/s11769-006-0026-1

Liang, J., Wang, M. J., Lu, J. A., Wang, M. J., Liang, J. Q., and Su, P. B. (2010). Logging Response Characteristics of Gas Hydrae Formation in Shenhu Area of the South China Sea. *Geoscience* 24 (3), 506–514. (In Chinese with English abstract). doi:10.3969/j.issn.1000-8527.2010.03.014

Liang, J., Wang, J. L., Lu, J. A., Kang, D. J., Kuang, Z. G., and Yang, C. Z. (2017a). The Logging Response Character and its Geological Significance of Gas Hydrae Formation in Taixinan Basin. *Earth Sci. Front.* 24 (4), 32–40. (In Chinese with English abstract). doi:10.13745/j.esf.yx.2016-12-32

Liang, J., Wang, J. L., Yang, C. Z., Kang, D. J., Lu, J. A., and Liang, J. Q. (2017b). Geophysical Characteristics of Gas Hydrate Bearing Sediments in the Eastern Sea Area of the Pearl River Mouth Basin. *Nat. Gas. Ind.* 37 (2), 126–133. (In Chinese with English abstract). doi:10.3787/j.issn.1000-0976.2017.02.017

Liang, J., Wang, M. J., Lu, J. A., Liang, J. Q., Wang, H. B., and Kuang, Z. G. (2013). Characteristics of Sonic and Seismic Velocities of Gas Hydrate Bearing Sediments in the Shenhu Area, Northern South China Sea. *Nat. Gas. Ind.* 33 (7), 29–35. (In Chinese with English abstract). doi:10.3787/j.issn.1000-0976.2013.07.005

Liang, J., Wang, M. J., Wang, H. B., Lu, J. A., and Liang, J. Q. (2009). Relationship between the Sonic Logging Velocity and Saturation for Gas Hydrate in Shenhu Area, Northern Slope of South China Sea. *Geoscience* 23 (2), 217–223. (In Chinese with English abstract). doi:10.3969/j.issn.1000-8527.2009.02.004

Liang, J., Zhang, W., Lu, J. a., Wei, J., Kuang, Z., and He, Y. (2019). Geological Occurrence and Accumulation Mechanism of Natural Gas Hydrates in the Eastern Qiongdongnan Basin of the South China Sea: Insights from Site GMGS5-W9-2018. *Mar. Geol.* 418, 106042. doi:10.1016/j.margeo.2019.106042

Lu, H. L., Kawasaki, T., Ukita, T., Moudrakovski, I., Fujii, T., Noguch, et al. (2011). Particle Size Effect on the Saturation of Methane Hydrate in Sediments — Constrained from Experimental Results. *Mar. Petroleum Geol.* 28 (10), 1805. doi:10.1016/j.marpetgeo.2010.11.007

Lu, J. A., Yang, S. X., Wu, N. Y., Zhang, G. X., Zhang, M., and Liang, J. Q. (2008). Well Logging Evaluation of Gas Hydrates in Shenhu Area, South China Sea. *Geoscience* 22 (3), 447–451. (In Chinese with English abstract). doi:10.1016/S1876-3804(08)60015-4

Meng, M., Liang, J., Lu, J., Zhang, W., Kuang, Z., Fang, Y., et al. (2021). Quaternary Deep-water Sedimentary Characteristics and its Relationship with Gas Hydrate Accumulations in the Qiongdongnan Basin, Northwest South China Sea. *Deep-sea Res. Part I* 177. doi:10.1016/j.dsr.2021.103628

Mo, X. W., Lu, J. A., Sha, Z. B., et al. (2008). A New Method for Gas Hydrate Saturation Estimation Using Well Logging Data. *J. Jilin Univ. (Earth Sci. Ed.* 42 (4), 921–927. (In Chinese with English abstract).

Paull, C. K., Ussler, W., and Dillon, W. P. (1991). Is the Extent of Glaciation Limited by Marine Gas-Hydrates? *Geophys. Res. Lett.* 18 (3), 432–434. doi:10.1029/91gl00351

Riedel, M., Collett, T. S., and Shankar, U. (2011). Documenting Channel Features Associated with Gas Hydrates in the Krishna-Godavari Basin, Offshore India. *Mar. Geol.* 279, 1–11. doi:10.1016/j.margeo.2010.10.008

Santamarina, J. C., Dai, S., Terzariol, M., Jang, J., Waite, W. F., Winters, W. J., et al. (2015). Hydro-bio-geomechanical Properties of Hydrate-Bearing Sediments from Nankai Trough. *Mar. Petroleum Geol.* 66, 434–450. doi:10.1016/j.marpetgeo.2015.02.033

Shukla, K. M., Kumar, P., Kumar, P., and Yadav, U. S. (2019). Gas Hydrate Reservoir Identification, Delineation, and Characterization in the Krishna-Godavari Basin Using Subsurface Geologic and Geophysical Data from the National Gas Hydrate Program 02 Expedition, Offshore India. *Mar. Petroleum Geol.* 108, 185–205. doi:10.1016/j.marpetgeo.2018.10.019

Su, M., Sha, Z., Zhang, C., Wang, H., Wu, N., Yang, R., et al. (2017). Types, Characteristics and Significances of Migrating Pathways of Gas-bearing Fluids in the Shenhu Area, Northern Continental Slope of the South China Sea. *Acta Geol. Sin. - Engl. Ed.* 91 (1), 219–231. doi:10.1111/1755-6724.13073

Su, P. B., Liang, J. Q., Peng, J., et al. (2018). *Petroleum Systems Modeling on Gas Hydrate of the First Experimental.*

Su, P. B., Liang, J. Q., Sha, Z. B., and Fu, S. Y. (2014). Gas Sources Condition of Gas Hydrate Formation in Shenhu Deep Water Sea Zone. *J. Southwest Petroleum Univ. Sci. &Technology Ed.* 36 (2), 1–8. (In Chinese with English abstract). doi:10.11885/j.issn.1674-5086.2013.10.16.01

Sua, P., Lianga, J., Peng, J., Zhang, W., and Xu, J. (2018). Petroleum Systems Modeling on Gas Hydrate of the First Experimental Exploitation Region in the Shenhu Area, Northern South China Sea. *J. Asian Earth Sci.* 168, 57–76. doi:10.1016/j.jseaes.2018.08.001

Walter, S. B., Charles, K. P., and William, U. (1999). Global and Local Variations of Interstitial Sulfate Gradients in Deep-Water, Continental Margin Sediments: Sensitivity to Underlying Methane and Gas Hydrates. *Mar. Geol.* 159 (1-4), 131–154. doi:10.1016/s0025-3227(99)00004-3

Wang, H. B., Liang, J., Gong, Y. H., Huang, Y. Y., Liu, X. W., and Sha, Z. B. (2005). Estimation of the Heat Flow in the Northern of the South China Sea Based on the Seismic Data of Gas Hydrate. *Geoscience* 19 (1), 67–73. (In Chinese with English abstract). doi:10.3969/j.issn.1000-8527.2005.01.010

Wang, X., Collett, T. S., Lee, M. W., Yang, S., Guo, Y., and Wu, S. (2014). Geological Controls on the Occurrence of Gas Hydrate from Core, Downhole Log, and Seismic Data in the Shenhu Area, South China Sea. *Mar. Geol.* 357, 272–292. doi:10.1016/j.margeo.2014.09.040

Wang, X. J., Wu, S. G., and Liu, X. W. (2006). Factors Affecting the Estimation of Gas Hydrate and Free Gas Saturation. *Chin. J. Geophys.* 49 (2), 505–511. doi:10.1002/cjg2.853

Wang, Z. W., Li, Z. B., and Liu, J. H. (2003). Logging Identification and Evaluation Methods for Gas Hydrates. *Mar. Geol. Quat. Geol.* 23 (2), 97–102. (In Chinese with English abstract).

Wu, N. Y., Zhang, H. Q., Yang, S. X., Liang, J. Q., and Wang, H. B. (2007). Preliminary Discussion on Natural Gas Hydrate (NGH) Reservoir System of Shenhu Area, Northern South China Sea. *Nat. Gas. Ind.* 27 (9), 1–6. (In Chinese with English abstract). doi:10.3321/j.issn:1000-0976.2007.09.001

Wu, S. G., Gong, Y. H., Mi, L. J., Wang, Z. J., and Wang, X. J. (2010). Study on Hydrocarbon Leakage System and Associated Gas Hydrate Reservoirs in the Deepwater Basin of Northern South China Sea. *Geoscience* 24 (3), 433–440. (In Chinese with English abstract). doi:10.3969/j.issn.1000-8527.2010.03.003

Yang, C. Z., Luo, K. W., Liang, J. Q., Lin, Z. X., Zhang, B. D., Liu, F., et al. (2020). Control Effect of Shallow-Burial Deepwater Deposits on Natural Gas Hydrate Accumulation in the Shenhu Sea Area of the Northern South China Sea. *Nat. Gas. Ind.* 40 (8), 68–76. (In Chinese with English abstract). doi:10.3787/j.issn.1000-0976.2020.08.005

Yang, S. X., Lei, Y., Liang, J. Q., Holland, M., Schultheiss, P., Lu, J. A., et al. (2017a). "Concentrated Gas Hydrate in the Shenhu Area, South China Sea: Results from Drilling Expeditions GMGS3 & GMGS4," in Proceedings of 9th International Conference on Gas Hydrates, Denver (Paper), 105.

Yang, S. X., Liang, J. Q., Lu, J. A., Qu, C. W., and Bo, L. (2017b). New Understandings on Characteristics and Controlling Factors of Gas Hydrate Reservoirs in Shenhu Area on Northern Slope of South China Sea. *Earth Sci. Front.* 24 (4), 1–14. (In Chinese with English abstract). doi:10.13745/j.esf.yx.2016-12-43

Yang, S. X., Zhang, M., Liang, J. Q., Lu, J. A., Zhang, Z. J., and Melanie, H. (2015). Preliminary Results of China's Third Gas Hydrate Drilling Expedition: A Critical Step from Discovery to Development in the South China Sea. *Fire Ice* 15 (2), 1–5.

Yu, X., Wang, J., Liang, J., Li, S., Zeng, X., and Li, W. (2014). Depositional Characteristics and Accumulation Model of Gas Hydrates in Northern South China Sea. *Mar. Petroleum Geol.* 56, 74–86. doi:10.1016/j.marpetgeo.2014.03.011

Zhang, G. X., Liang, J. Q., Lu, J. A., Yang, S. X., Zhang, M., Xin, S., et al. (2014). Characteristics of Natural Gas Hydrate Reservoirs on the Northeastern Slope of the South China Sea. *Nat. Gas. Ind.* 34 (11), 1–10. (In Chinese with English abstract). doi:10.3787/j.issn.1000-0976.2014.11.001

Zhang, W., Liang, J., Lu, J. a., Wei, J., Su, P., Fang, Y., et al. (2017). Accumulation Features and Mechanisms of High Saturation Natural Gas Hydrate in Shenhu Area, Northern South China Sea. *Petroleum Explor. Dev.* 44 (5), 708–719. doi:10.1016/s1876-3804(17)30082-4

Zhang, W., Liang, J. Q., Su, P. B., Wei, J. G., Sha, Z. B., Lin, L., et al. (2018). Migrating Pathways of Hydrocarbons and Their Controlling Effects Associated with High Saturation Gas Hydrate in Shenhu Area, Northern South China Sea. *Geol. China* 45 (1), 1–14. (In Chinese with English abstract). doi:10.12029/gc20180101

Zhang, W., Liang, J., Wan, Z., Su, P., Huang, W., Wang, L., et al. (2020). Dynamic Accumulation of Gas Hydrates Associated with the Channel-Levee System in the Shenhu Area, Northern South China Sea. *Mar. Petroleum Geol.* 117, 104354. doi:10.1016/j.marpetgeo.2020.104354

Zhong, G., Liang, J., Guo, Y., Kuang, Z., Su, P., and Lin, L. (2017). Integrated Core-Log Facies Analysis and Depositional Model of the Gas Hydrate-Bearing Sediments in the Northeastern Continental Slope, South China Sea. *Mar. Petroleum Geol.* 86, 1159–1172. doi:10.1016/j.marpetgeo.2017.07.012

Conflict of Interest: The authors declare that the research was conducted in the absence of any commercial or financial relationships that could be construed as a potential conflict of interest.

Publisher's Note: All claims expressed in this article are solely those of the authors and do not necessarily represent those of their affiliated organizations, or those of the publisher, the editors and the reviewers. Any product that may be evaluated in this article, or claim that may be made by its manufacturer, is not guaranteed or endorsed by the publisher.